

Determination of Critical Energy Release Rates for Discrete Damage Mechanics Analysis in ANSYS

E.J. Barbero¹ and M. Shahbazi²,
West Virginia University, Morgantown USA

Abstract

Matrix cracks are the first type of degradation observed in most polymer matrix composites. The Discrete Damage Mechanics (DDM) model has been added to ANSYS[®] as a user material (UserMAT) to enable prediction of initiation and evolution of matrix cracks in laminated composites. Besides the usual material properties that describe the elasticity and strength of a ply, DDM uses two, in situ, critical energy release rates (GIc and GIIc) to provide accurate predictions of intralaminar cracking. No standard test method exists to determine these properties in situ, in a finished laminate. Therefore, a methodology is proposed herein to evaluate these properties in terms of experimental stiffness-degradation data from specimens made with two different laminate stacking sequences. Experimental data for other stacking sequences of the same material system are used to validate the methodology. Comparison with other model-results are also presented. The objectivity of the constitutive model is evaluated by performing both p- and h-refinement.

1 Introduction

Crack initiation and propagation in composite materials are of particular importance for the design, production, certification, and monitoring of an increasingly large variety of structures. In [1], the response of each lamina is obtained from a meso-model that couples the behavior of a single layer and an interlaminar layer. The first layer uses a damage model that takes into account the effects of transverse matrix crack. The second layer uses a damage model that takes into account delaminations. Parameter identification and validation with open-hole tensile tests on quasi-isotropic laminates is described in [2].

¹Professor. Corresponding author: ever.barbero@mail.wvu.edu.

²Graduate Research Assistant.

The final publication is available at <http://dx.doi.org/10.1016/j.tafmec.2017.05.016>

Another approach to simulate the onset and propagation of transverse matrix cracking, as well as other failure mechanisms, is serial-parallel mixing theory [3–5]. This formulation obtains the composite response from the constitutive performance of its constituents, usually matrix and fiber, each one of them simulated with its own constitutive law. With this theory it is possible to use any given non-linear material model, such as damage or plasticity, to characterize the composite components.

Most of the models developed specifically to address the phenomenon of transverse matrix cracking establish a relation between the available strain energy of the material and the density of matrix cracks [6–12]. Following this approach, [13] uses finite fracture mechanics to obtain the energy release rate required to double the crack density, with the apparition of a new crack between two existing cracks. This model was improved with the concept of incremental and continuous variation of crack density [10]. Similarly, the equivalent constrained model (ECM) [11, 14], defines a law that provides the evolution of stiffness as matrix crack density increases.

Some of the above mentioned formulations provide analytical expressions that can be used to obtain the mechanical response for simple geometry and load configurations. However, it is often necessary to include the constitutive model into Finite Element Analysis (FEA) software. Some models have been included in commercial FEM software [15, 16]. Others that are available as plugins for existing FEA software [17, 18], or as user programmable features, including UMAT, UGENS and UserMAT [19].

The discrete damage mechanics (DDM) material model can be incorporated as a user material [19, UserMAT] in ANSYS Mechanical APDL (MAPDL) [20, Ch. 9]. Furthermore, ANSYS Workbench allows optimization of any set of variables to any user defined objective defined in a MAPDL by importing the APDL script into Workbench and using Design Explorer (DE) tools [21]. In this way, DDM is available for Design Exploration, where the designer can optimize the structure taking into account crack initiation, stress redistribution, stiffness degradation, and crack density evolution (which may affect the permeability of the laminate). In this way, design optimization and sensitivity of various performance metrics to any design variable can be easily done while taking into account the response of the cracked structure.

Although elastic moduli are available for many composite material systems, the invariant material properties required by DDM model are only available for a few material systems. However, laminate modulus and Poissons ratio degradation of laminated composites as a function of applied strain are available for several material systems [22, 23]. This study shows how to use available data to infer the material properties required by DDM model. Specifically, the main purpose of this study is to find the in situ critical value of the energy release rate (ERR) in opening mode G_{Ic} and critical value of ERR in shear mode G_{IIc} from macro-scale tensile data, which is easy to obtain. Once G_{Ic} , G_{IIc} , are known for the material system (composite lamina) of interest, DDM can be used in ANSYS to predict intralaminar cracking initiation and evolution of laminated composite structures built with the same material system.

The stated objective is achieved by minimizing the error between DDM model predictions and available experimental data. Once the input properties G_{Ic} and G_{IIc} are found, the accuracy of DDM predictions is checked by comparing those predictions with experimental data for other laminates that have not been used to fit the input properties. Although the input properties are fitted using a specific mesh (one element) and type of element (PLANE 182), the DDM user material constitutive model is mesh- and element-type insensitive; that is, the DDM constitutive model possesses *objectivity*. Mesh sensitivity is assessed in this work by performing both p- and h-refinement.

2 Model Formulation

The discrete damage mechanics (DDM) model is a semi-analytical linear-elastic fracture mechanics (LEFM) model [24]. The model is able to predict the crack density $\lambda = 1/2l$, simultaneously in all laminae of a laminate, where $2l$ is the distance between each pair of cracks, as shown in Figure 1.

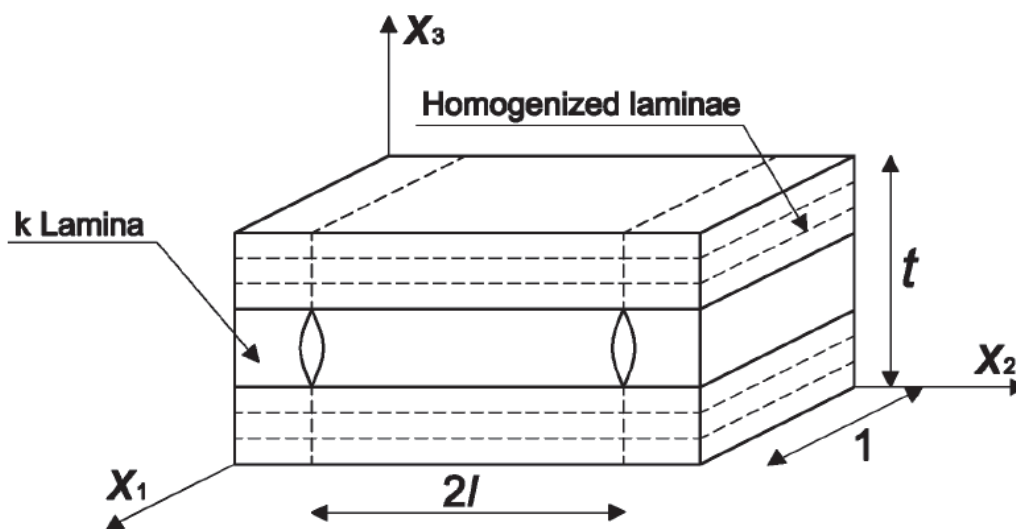


Figure 1: Representative Volume Element used by Discrete Damage Mechanics.

By increasing the strain ϵ_x , DDM updates the state variables (crack density λ), and calculates the shell stress resultants N, M , and tangent stiffness matrix A_T, B_T, D_T , as functions of crack density. Thus, the state variable of the constitutive model is an array containing the crack density for all laminae at an integration point of the shell element. Since energy release rates (ERR) are used to predict damage initiation, DDM does not need

in situ correction of strength. In fact, the critical ERR values can be used to calculate the in situ strength [25, (4.99),(4.113)]. Determination of in situ critical ERR values using macro-scale test data is the main the objective of this work.

In laminated composites, matrix cracks grow parallel to the fiber orientation due to the inability of the crack front to break the fibers. These cracks reduce the stiffness of the cracked lamina, which then sheds its share of the load onto the remaining laminas. Since the actual geometry of the cracks is modeled, the formulation is called *discrete damage mechanics* (DDM).

The basic ingredients of the DDM model for transverse tension and in-plane shear damage are listed below:

- i. In each lamina, the state variable is the crack density λ .
- ii. The independent variable is the midsurface strain $\epsilon = \{\epsilon_1, \epsilon_2, \gamma_6\}^T$.
- iii. The damage activation function is

$$g = (1 - r) \sqrt{\frac{G_I(\lambda, \epsilon)}{G_{Ic}}} + r \frac{G_I(\lambda, \epsilon)}{G_{Ic}} + \frac{G_{II}(\lambda, \epsilon)}{G_{IIc}} - 1 \leq 0$$

$$r = \frac{G_{Ic}}{G_{IIc}} \quad (1)$$

- iv. The damage threshold is represented by the material properties G_{Ic}, G_{IIc} . Before cracking starts, $\lambda = 0$ and (1) is a damage initiation criterion [26]. With $\lambda = 0$, the strain for which g reaches zero is the strain for crack initiation. Once cracking starts, (1) becomes a damage activation function by virtue of the automatic hardening described below (v).
- v. For a given value of strain, the calculated values of energy release rate $G_I(\lambda), G_{II}(\lambda)$ are monotonically decreasing functions of λ , as it can be inferred from (14–15) because $Q^{(k)}$ are monotonically decreasing functions of λ . Therefore, as soon as λ grows, $g < 0$, stopping further damage until the strain is increased.
- vi. By virtue of (v), no damage evolution function is needed. The crack density λ is thus adjusted to set the laminate in equilibrium with the external loads for the current strain while satisfying $g = 0$, using a return mapping algorithm [27, Chapter 8].
- vii. Crack density grows until saturation, defined as $\lambda_{lim} = 1/t_k$, where t_k is the thickness of lamina k .

The solution begins by calculating the reduced stiffness of the laminate $[C] = [A]/h$ for a given set of crack densities λ , where $[A]$ is the in-plane laminate stiffness matrix, and

h is the thickness of the laminate. For a symmetric laminate under membrane loads and assuming the laminae to be thin, we have

$$\begin{aligned}\frac{\partial w^i}{\partial x} &= \frac{\partial w^i}{\partial y} = 0 \\ \sigma_z^i &= 0\end{aligned}\quad (2)$$

where $u(x, y, z), v(x, y, z), w(x, y, z)$, are the displacements of a point in lamina i as a function of the coordinates x, y, z . For thin laminae the cracks occupy the entire thickness of the lamina and it suffices to work with thickness averages of the variables. A thickness average is denoted by

$$\hat{\phi}_i(x, y) = \frac{1}{t_i} \int_{t_i} \phi_i(x, y, z) dz \quad (3)$$

where t_i denotes the thickness of lamina i . Specifically,

- $\hat{u}^i(x, y), \hat{v}^i(x, y), \hat{w}^i(x, y)$, are the thickness-average displacements in lamina i as a function of the in-plane coordinates x, y .
- $\hat{\epsilon}_1^i(x, y), \hat{\epsilon}_2^i(x, y), \hat{\gamma}_6^i(x, y)$, are the thickness-average strains in lamina i .
- $\hat{\sigma}_1^i(x, y), \hat{\sigma}_2^i(x, y), \hat{\sigma}_6^i(x, y)$, are the thickness-average stress in lamina i .

Out-of-plane (intralaminar) shear stress components appear due to the perturbation of the displacement field caused by the crack. These are approximated by linear functions through the thickness of the i -lamina

$$\begin{aligned}\sigma_4^i(z) &= \sigma_4(z_{i-1}) + [\sigma_4(z_i) - \sigma_4(z_{i-1})] \frac{z - z_{i-1}}{t_i} \\ \sigma_5^i(z) &= \sigma_5(z_{i-1}) + [\sigma_5(z_i) - \sigma_5(z_{i-1})] \frac{z - z_{i-1}}{t_i}\end{aligned}\quad (4)$$

where z_{i-1} and z_i are the thickness coordinate at the bottom and top of lamina i , respectively.

To solve for the average displacements $\hat{u}^i(x, y), \hat{v}^i(x, y)$, in all laminae i for a given crack density λ and applied strain ϵ , the in-plane and intralaminar equilibrium equations, the kinematic equations, and the constitutive equations are invoked [24]. This leads to a system of $2n$ partial differential equations in $\hat{u}^i(x, y), \hat{v}^i(x, y)$, which has a particular solution of the form

$$\begin{aligned}\hat{u}^i &= a^i \sinh \lambda y + ax + by \\ \hat{v}^i &= b^i \sinh \lambda y + bx + cy\end{aligned}\quad (5)$$

and substituted into the PDE system leads to an eigenvalue problem

$$([K] - \eta_e^2[M]) \begin{Bmatrix} a^i \\ b^i \end{Bmatrix}_e = \{0\} \quad (6)$$

where η are the $2n$ eigenvalues, $\{a^i, b^i\}_e^T$ are the $2n$ eigenvectors, and n is the number of laminae in the laminate. Since always two of the eigenvalues are zero, the general solution of the PDE system is built as the linear combination of $2n - 2$ independent solutions as follows

$$\begin{Bmatrix} \hat{u}^i \\ \hat{v}^i \end{Bmatrix} = \sum_{e=1}^{2n-2} \alpha_e \begin{Bmatrix} a^i \\ b^i \end{Bmatrix}_e \sinh \eta_e y + \begin{Bmatrix} a \\ b \end{Bmatrix} x + \begin{Bmatrix} b \\ c \end{Bmatrix} y \quad (7)$$

where α_e are unknown coefficients in the linear combination. The general solution contains $2n + 1$ unknown coefficients, including a, b, c , and α_e with $e = 1 \dots 2n - 2$. To determine these coefficients, one needs $2n + 1$ boundary conditions on the boundary of the representative volume element (RVE) in Figure 1. Note that the RVE spans a unit length along the fiber direction x , a distance $2l$ between successive cracks (along y) and the whole thickness h of the symmetric laminate.

The crack density enters into the solution through the length of the RVE, i.e., $2l = 1/\lambda$. The applied stress (or strain) enters through force equilibrium on the RVE. This results in $2n + 1$ boundary conditions on a system of $2n + 1$ algebraic equations that can be solved for the $2n + 1$ coefficients in (7), to obtain the average displacements in all laminae from (7) for given values of crack density λ and applied load $\hat{\sigma} = N/h$.

The thickness-averaged strain field in all laminae can now be obtained by using the kinematic equations, i.e., by direct differentiation of (7)

$$\hat{\epsilon}_x^i = \frac{\partial \hat{u}^i}{\partial x} \quad ; \quad \hat{\epsilon}_y^i = \frac{\partial \hat{v}^i}{\partial y} \quad ; \quad \hat{\gamma}_{xy}^i = \frac{\partial \hat{u}^i}{\partial y} + \frac{\partial \hat{v}^i}{\partial x} \quad (8)$$

The compliance S and CTE α of the laminate in the coordinate system of lamina k (x, y , Figure 1) can be calculated one column at a time by solving for the strains (8) for four load cases, as follows

$${}^a \hat{\sigma} = \begin{Bmatrix} 1 \\ 0 \\ 0 \end{Bmatrix}_{\Delta T=0} \quad {}^b \hat{\sigma} = \begin{Bmatrix} 0 \\ 1 \\ 0 \end{Bmatrix}_{\Delta T=0} \quad {}^c \hat{\sigma} = \begin{Bmatrix} 0 \\ 0 \\ 1 \end{Bmatrix}_{\Delta T=0} \quad {}^d \hat{\sigma} = \begin{Bmatrix} 0 \\ 0 \\ 0 \end{Bmatrix}_{\Delta T=1} \quad (9)$$

Cases a, b, c , provide one column each for the compliance matrix of the damaged laminate

$$S = \begin{bmatrix} {}^a \epsilon_x & {}^b \epsilon_x & {}^c \epsilon_x \\ {}^a \epsilon_y & {}^b \epsilon_y & {}^c \epsilon_y \\ {}^a \gamma_{xy} & {}^b \gamma_{xy} & {}^c \gamma_{xy} \end{bmatrix} \quad (10)$$

and case d ($\Delta T = 1$) provides the CTE of the damaged laminate. Next, the laminate stiffness in the coordinate system of lamina k is

$$C = S^{-1} \quad (11)$$

The laminate stiffness is defined by the contribution of the cracking lamina k plus the contribution of the remaining $n - 1$ laminas, as follows

$$C = Q^k \frac{t_k}{h} + \sum_{m=1}^n (1 - \delta_{mk}) Q^m \frac{t_m}{h} \quad (12)$$

where the Kronecker *delta* is defined as $\delta_{mk} = 1$ if $m = k$, otherwise 0. The left-hand side (LHS) of (12) is known from (11) and all values of Q^m can be easily calculated since the m laminas are not cracking at the moment. Therefore, one can calculate the reduced stiffness Q^k of the cracking lamina k as follows

$$Q^k = \frac{h}{t_k} \left[C - \sum_{m=1}^n (1 - \delta_{mk}) Q^m \frac{t_m}{h} \right] \quad (13)$$

2.1 Fracture Energy

Under displacement control, the energy release rate (ERR) is defined as the partial derivative of the strain energy U with respect to the crack area A_c . Mode decomposition [28] can be accomplished as follows

$$\begin{aligned} U_I &= \frac{V_{RVE}}{2h} \sum_{k=1}^n t_k (\epsilon_2 - \tilde{\alpha}_2^{(k)} \delta T) Q_{2j}^{(k)} (\epsilon_j - \tilde{\alpha}_j^{(k)} \delta T) \\ U_{II} &= \frac{V_{RVE}}{2h} \sum_{k=1}^n t_k (\epsilon_6 - \tilde{\alpha}_6^{(k)} \delta T) Q_{6j}^{(k)} (\epsilon_j - \tilde{\alpha}_j^{(k)} \delta T) \end{aligned} \quad (14)$$

where $h = \sum_{k=1}^n t_k$, $\epsilon_6 = \gamma_{12}$, and $\tilde{\alpha}^{(k)}$ are the CTE of lamina k . Equation (14) is cast in the coordinate system of the cracking lamina ($k = c$) so that ϵ_2 is mode I (crack opening) and ϵ_6 is mode II (crack shear).

According to experimental observations on laminated, brittle matrix composites (e.g., using most toughened epoxy matrices), cracks develop suddenly over a finite length, and thus are not infinitesimal. Then, Griffith's energy principle is applied on its discrete (finite) form in order to describe the observed, discrete (finite) behavior of crack growth, as follows

$$\begin{aligned} G_I &= 2\gamma_I = \frac{U_{Ia} - U_{Ib}}{2t_c} \\ G_{II} &= 2\gamma_{II} = \frac{U_{IIa} - U_{IIb}}{2t_c} \end{aligned} \quad (15)$$

where $U_{Ia}, U_{Ib}, U_{IIa}, U_{IIb}$, are the elastic strain energies in modes I and II, for crack densities λ_a and $\lambda_b = 2\lambda_a$, and $\Delta A_c = 2t_c \times 1$ is the increment of crack area when a new crack propagates in two symmetrically located laminas, each with thickness t_c , in and RVE with dimension 1 along the fiber direction.

For the current damage state i , characterized by crack density (state variable) $\lambda_i = 1/(2l)$, the RVE in Figure 1 has thickness h , a unit length along the crack direction x , and width $2l$ (between cracks), resulting in a volume $V_{RVE} = h/\lambda$. Due to shear lag, every new crack appears between two existing cracks, yielding new crack spacing l , new crack density $\lambda_{i+1} = 2\lambda_i$ and newly created area $\Delta A_c = 2t_c$.

The damage activation function (1) can now be calculated for any value of λ and applied strain $\epsilon_x, \epsilon_y, \gamma_{xy}$. Note that the computation of the ERR components derives directly from the displacement solution (7) for a discrete crack (Figure 1). When this formulation is used along with the finite element method (FEM), it does not display mesh dependency on the solution and does not require the arbitrary specification of a characteristic length [29,30], in contrast to formulations based on smeared crack approximations. A shell element capable of utilizing this formulation is implemented as a user element into ANSYS [27,30]. Abaqus implementation is available as a User General Section (UGENS) in [31]. Additional details are given in [24,32–36].

3 Methodology

In this work, Design Optimization (DO) is used to adjust the values of G_{Ic} and G_{IIc} so that the DDM prediction of laminate response closely approximates the experimental data. Design Optimization tools can be found in ANSYS Workbench in the Design Explorer (DE) module [21], which includes also Design of Experiments (DoE), Properties Correlation (PC), Response Surface (RS), Response Surface Optimization (RSO), and Six Sigma Analysis.

First, we use DoE to identify the laminates that are most sensitive to each material property. The focus at this point is to determine the minimum number of laminates to be used in the experiments that are needed to adjust the material properties. As a result, we identify two laminates that are the most sensitive to the material properties sought. Additional experiments conducted with other laminate stacking sequences (LSS) are not used to adjust properties but to assess the quality of the predictions.

The objective function is the error between the predictions and the experimental data. Given N experimental values of laminate modulus $E(\epsilon_i)$, where ϵ is the strain applied to the laminate, and $i = 1 \dots N$, the error D is defined as

$$D = \frac{1}{N} \sqrt{\sum_{i=1}^N \left(\left. \frac{E}{E_0} \right|_{\epsilon=\epsilon_i}^{\text{DDM}} - \left. \frac{E}{E_0} \right|_{\epsilon=\epsilon_i}^{\text{Experimental}} \right)^2} \quad (16)$$

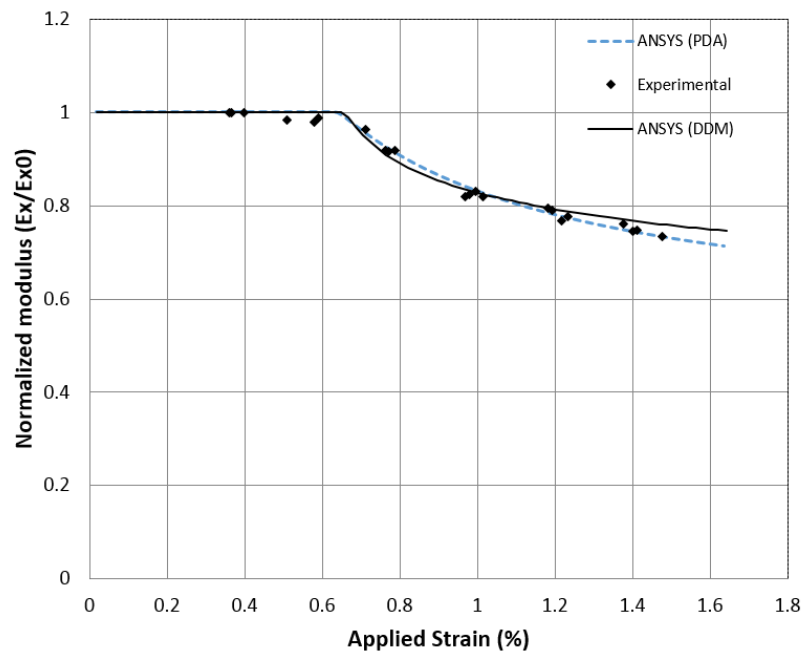


Figure 2: Normalized modulus vs. applied strain for laminate #1 (Table 2).

where E, E_0 , are the cracked and virgin moduli of the laminate, respectively, and N is the number of data points available for ϵ_i values of applied strain. For example, a set of experimental data points are shown in Figure 2.

Let's denote the input properties by the array $X = \{G_{Ic}, G_{IIc}\}$. The objective function $D = D(X)$ can be calculated by evaluation of (16) through execution of the finite element analysis (FEA) code for N values of strain. Each FEA analysis is controlled by the APDL script, which calls for the evaluation of the non-linear response of the damaging laminate for each value of strain, with properties X . The APDL script is explained in Section 4.1.

An alternative to direct evaluation of the objective function is to approximate it with a multivariate quadratic polynomial. The approximation is called response surface (RS). It can be constructed with only few actual evaluations of the objective by choosing a small number of sampling points for the input. The sampling points are chosen using Design of Experiments (DoE) theory. The number of evaluations needed to construct the response surface (RS) and to find an optimum by direct optimization (DO) are shown in Table 1.

The shape of the RS can be inferred by observing the variation of the objective D as a function of only one input at a time as shown in Figure 3 and 4. The abscissa spans each of the inputs and the ordinate measures the error (16) between predicted and experimental data. The sensitivity of G_{IIc} for laminate #1 (Figure 4) is negligible, of order 10^{-7} , because the laminas are not subject to shear. Therefore, the experimental data of laminate #1 is

Table 1: Number of FEA evaluations used (a) to construct the response surface (RS) and (b) to adjust the input properties by direct optimization (DO).

# of inputs	Inputs	Number of evaluations	
		RS (Response Surface)	DO (Adaptive Single-Objective)
1	G_{Ic}	5	9
2	G_{Ic}, G_{IIc}	9	21

used to evaluate only G_{Ic} . Since the laminas at ± 40 in laminate #8 experience both traction shear, laminae #8 is used to evaluate G_{IIc} while maintaining G_{Ic} constant at the value found previously with laminate #1.

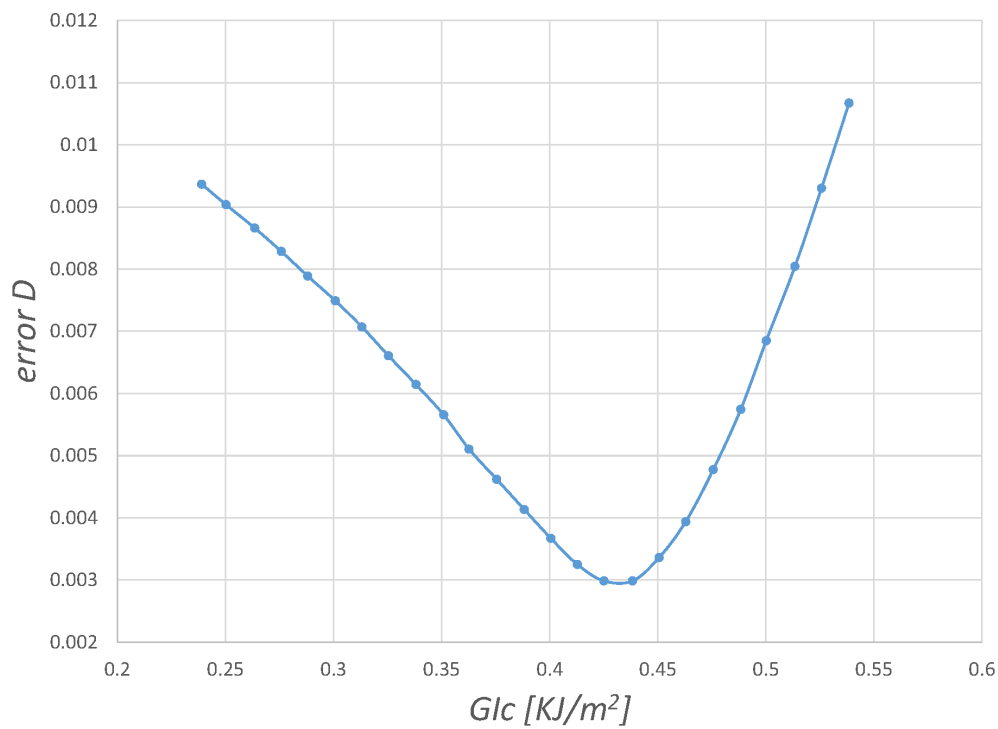


Figure 3: Response surface chart. Error D vs. G_{Ic} for laminate #1 (Table 2) with input ranges given in Table 3.

The RS is multivariate quadratic polynomial that approximates the objective function $D_{RS} = f(X_i)$ as a function of the input variables. The sensitivity S of the objective D to

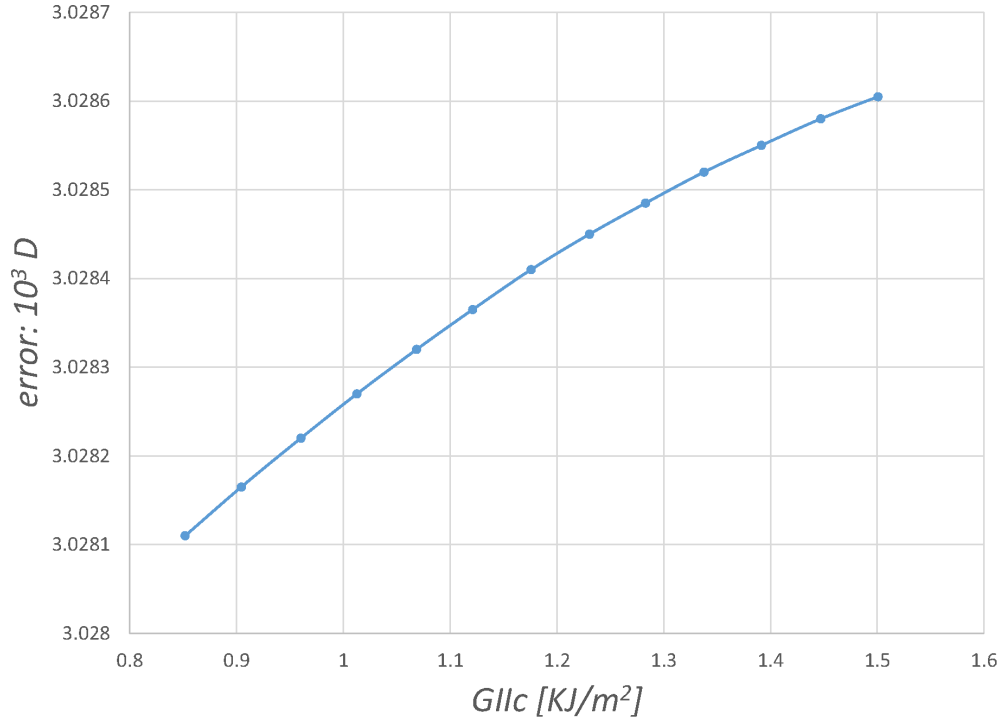


Figure 4: Response surface chart. Error ($10^3 \times D$) vs. G_{IIc} for laminate #1 (Table 2) with input ranges given in Table 3.

input X in the user specified interval $[X_{min}, X_{max}]$ is calculated as

$$S = \frac{\max(D) - \min(D)}{\text{average}(D)} \quad (17)$$

and tabulated in Table 3. Note that the sensitivity can be calculated from the error evaluated directly from FEA analysis or from the RS. The latter is much more expedient than the former, as shown in Table 1 by the number of evaluations needed.

Two optimization techniques are used in this work: Response Surface (RS) and Adaptive Single-Objective.

When the objective function is approximated by a RS, finding the minimum is expedient because the RS is a multivariate quadratic polynomial, for which the minimum can be found with little computational effort. The only significant computational cost is to construct the RS, for which actual FEA evaluation of the objective function is needed at a number of points chosen by Design of Experiments (DoE) theory. While RS optimization is fast, its accuracy is limited by the quality of the RS built using DoE within the response domain specified by the user as “Input range” in Table 3.

Table 2: Laminate stacking sequence for all laminates for which experimental data is available.

Laminate #	LSS
1	$[0_2/90_4]_S$
2	$[\pm 15/90_4]_S$
3	$[\pm 30/90_4]_S$
4	$[\pm 40/90_4]_S$
5	$[0/90_8/0_{1/2}]_S$
6	$[0/\pm 70_4/0_{1/2}]_S$
7	$[0/\pm 55_4/0_{1/2}]_S$
8	$[0/\pm 40_4/0_{1/2}]_S$
9	$[0/\pm 25_4/0_{1/2}]_S$

Table 3: Sensitivity S of the objective (error) to each input (property).

Input	Input range		Error D			Sensitivity	Laminate
	min(Input)	max(Input)	min(D)	max(D)	ave(D)	S	
G_{Ic}	0.3	0.6	0.0019	0.0096	0.00542	1.4136	#1
G_{IIc}	0.9	1.5	0.02524	0.0379	0.03007	0.42101	#8

Adaptive Single-Objective optimization [21] is a gradient-type minimization, using the MISQP algorithm, acting on a Kriging response surface, while the response domain is reduced incrementally to find the global minimum. The Kriging response surface (KRS) is built using FEA evaluations of the objective function at a number of points chosen by an optimal space-filling design of experiments algorithm. A new KRS is built after each domain reduction keeping the previous information and adding new evaluations inside the new smaller domain. Thus, the RS is increasingly accurate but it tends to require more FEA evaluations (Table 1), which increases the solution time.

4 Determination of Material Properties

The material properties (which are the *input* to the optimization) can be adjusted with any mesh and any type of elements that represent the gage section of the specimen, or a single element to represent a single material point of the specimen. For expediency, a single linear element (PLANE 182) is used in this study.

4.1 APDL

ANSYS Parametric Design Language is used by ANSYS Mechanical [19]. The APDL script is used to call the user material (*USERMATLib.DLL* [20, Ch. 9]), specify the geometry,

Table 4: Lamina elastic properties and in situ strength values.

Property	Units	Value	Ref.
E_1	MPa	44700	[22]
E_2	MPa	12700	[22]
G_{12}	MPa	5800	[22]
ν_{12}	-	0.297	[22]
ν_{23}	-	0.411	[22]
G_{Ic}	KJ/m^2	0.254	guess value
G_{IIc}	KJ/m^2	1.4	guess value
CTE_1	MPa	3.7	[25]
CTE_2	MPa	30	[25]
ΔT	MPa	0	[25]
Ply thickness	mm	0.144	[23]

mesh, boundary conditions, and the strain applied to the laminate. The latter is specified by imposing a specified displacement, to mimic the experiment, which is available for a finite set of values of applied strain.

In APDL, parameters can be defined dynamically, i.e., simply by providing values for them, as follows:

```

/TITLE, Laminate #1, USERMATLib.DLL
/PREP7                               ! Start pre-processor module
!=== PARAMETERS =====
L0 = 0.02                             ! initial the crack density [cracks/mm]
ShellDimensionX = 55.0                ! model dimensions [mm]
ShellDimensionY = 10.0                ! mm
tk = .144                             ! ply thickness [mm]
NL = 2                                ! number layers half laminate
Nprops = 3+9*NL                       ! # material properties and LSS
!=== VALUES FOR TBDATA =====
GIc = 0.254                           ! initial value
GIIc = 1.400                          ! initial value
deltaT = 0.0                          ! degrees C
E1 = 44700                             ! MPa
E2 = 12700                             ! MPa
G12= 5800                             ! MPa
nu12 = 0.297                          !
nu23 = 0.410                          !
CTE1 = 3.7                             ! microstrains
CTE2 = 30.0                           ! microstrains

```

All the parameters defined in APDL can be designated as **design variables** (called *inputs* in the terminology used by Workbench's Design Explorer [21]), or become compo-

nents of the **objective function** (called *outputs* in Design Explorer). In this work the *inputs* are the material properties being sought (G_{Ic} and G_{IIc}) and the only *output* is the error D calculated as in (16). By minimizing the error, we can adjust the values of the material properties.

The DDM UserMATLib.DLL R14 available in [37], is documented in [20]. It works with ANSYS R14, 15, 16, and 17. It uses $Nprops = 3 + 9 * NL$ parameters that include 3 laminate material properties ($G_{Ic}, G_{IIc}, \Delta T$) and 9 parameters per lamina, including 7 material properties ($E_1, E_2, G_{12}, \nu_{12}, \nu_{23}, CTE_1, CTE_2$), plus angle and thickness. The laminate must be symmetric and NL is the number of laminas in the symmetric half of the laminate. The values of G_{Ic} and G_{IIc} in Table 4 are initial (guess) values for the optimization. The material properties (Table 4) and the laminate stacking sequence (Table 2) are entered as TBDATA, as follows. Note that all the variable names refer to their definitions above.

```
!=== USERMAT DECLARATION SECTION =====
TB,USER,1,1,Nprops,      ! DECLARES USAGE OF USERMAT 1, MAT 1,
TBTEMP,0                ! ref. temperature
TBDATA,,GIc,GIIC,detaT,E1,E2,G12      ! 6 values per TBDATA line
TBDATA,,nu12,nu23,CTE1,CTE2,0,2*tk
TBDATA,,E1,E2,G12,nu12,nu23,CTE1
TBDATA,,CTE2,90,4*tk,
TB,STAT,1,,3*NL        ! NUMBER OF STATE VARIABLES
! INITIALIZE THE STATE VARIABLES
TBDATA,,L0,L0,L0,L0,L0,L0
```

DDM UserMATLib.DLL R14 uses $3*NL$ state variables ($\lambda, D_2(\lambda), D_6(\lambda)$) as explained in [20, Ex. 9.1]. Only the crack density in every lamina λ are true state variables. $D_2(\lambda)$ and $D_6(\lambda)$ are continuum damage parameters, derived from λ , that are stored for every Gauss point (for convenience) because they allow for a quick calculation of the reduced stiffness $[Q]^{(k)}$ for each lamina, which is a function of crack density, as follows

$$[Q]^{(k)} = \begin{bmatrix} \tilde{Q}_{11}^{(k)} & (1 - D_2)\tilde{Q}_{12}^{(k)} & 0 \\ (1 - D_2)\tilde{Q}_{12}^{(k)} & (1 - D_2)\tilde{Q}_{22}^{(k)} & 0 \\ 0 & 0 & (1 - D_6)\tilde{Q}_{11}^{(k)} \end{bmatrix} \quad (18)$$

in terms of the virgin lamina stiffness $[\tilde{Q}]^{(k)}$.

The true state variables must be initialized (via TBDATA) to values that are representative of the initial defects that are always present in any composite. The results are not sensitive to the value chosen as long as the value is small (0.02 crack/mm in this study).

After the material properties and laminate stacking sequence are defined, the analyst is free to introduce whatever geometry, loads, and boundary conditions are needed to represent the problem at hand, as it is normally done in ANSYS or any other FEA package.

The ensuing discussion illustrates the case of a ASTM D 3039 rectangular specimen subject to a ramped displacement at one end to simulate the load. Symmetry is assumed at the midspan of the specimen.

The mesh and solution phases are defined in the usual way. The strain is applied as a displacement on the boundary, which is subdivided into substeps to mimic the available experimental data:

```
!=== MESH =====
ET,1,182,,3          ! PLANE182, plane elements with plane stress
R,1,2*6*tk          ! Real const. 1, thickness of whole laminate
N,1                  ! Define node 1, coordinates=0,0,0
N,2,ShellDimensionX,0 ! Define node 2,
N,3,ShellDimensionX,ShellDimensionY
N,4,0,ShellDimensionY
E,1,2,3,4           ! Generate element 1 by node 1 to 4
FINISH              ! Exit pre-processor module
!=== SOLUTION =====
/SOLU               ! Start Solution module
ANTYPE,STATIC
OUTRES,ALL,1       ! Store results for each substep
D,1,all            ! Define b.c. on node 1, totally fixed
D,2,UY,0.00
D,2,UX,1.05        ! Define b.c. on node 2, Uy=0.0
D,3,UX,1.05        ! Define displacement on node 3, Ux=0.1
D,4,UX,0.00        ! Define b.c. on node 4, Ux=0.0
NSUBST,100,200,100 ! 100 = Number of substeps in this load step
SOLVE              ! Solve load step
FINISH            ! Exit solution module
```

The error (16) is calculated in the post-processing phase. The laminate modulus $E_x(\lambda)$ decreases as a function of crack density λ . To calculate the reduced modulus, we need to get displacements ($VGET,UX3,2,0$) and reactions ($VGET,FX4,3,0$ and $VGET,FX1,4,0$) as a function of applied strain. In this example we have 100 substeps and $NDA=22$ experimental data points. For each experimental data point, a loop scans the substeps to find the one that has the strain closest to the experimental, in order to compute each term in the summation (16). The accumulated error is stored in D , which will be designated in WorkBench Design Explorer as the *output* for optimization.

```
! === CALCULATE THE ERROR =====
/POST26             ! Start time-historic post-process
NSOL,2,3,U,X, UXnode3 ! Load displacements node 3
RFORCE,3,4,F,X,FXnode4 ! Load reaction force node 4
RFORCE,4,1,F,X,FXnode1 ! Load reaction force node 1
LINES,1000
PRVAR,2,3,4        ! list displacements and reactions
```

```

NDATA=22
*DIM,AA,ARRAY,NDATA,2,1, , ,
*SET,AA(1,1,1) , 0.35909 ! first data point strain
*SET,AA(1,2,1) , 1 ! first data point modulus
...
*SET,AA(22,1,1) , 1.47645 ! last data point strain
*SET,AA(22,2,1) , 0.733498 ! last data point modulus

VGET,UX3,2,0
VGET,FX4,3,0
VGET,FX1,4,0

*SET,L,0
*DO,I,1,NDATA,1
*DO,J,1,100,1
  SXP=AA(I,1,1)
  EEXP=AA(I,2,1)
  SCS=1.8181*UX3(J,1)
  FN4=FX4(J,1)
  FN1=FX1(J,1)
  FN2=FX1(2,1)
  SCS2=1.8181*UX3(2,1)
  MRG=ABS((SCS-SXP))
  *IF,MRG,LE,0.009545,THEN
    NUM=((FN1+FN4)*(SCS2))
    DEN=2*(FN2)*(SCS)
    EPE=NUM/DEN
    ER1=EPE-EEXP
    ER2=ER1*ER1
    L=L+ER2
  *ENDIF
*ENDDO
*ENDDO
D=(1/NDATA)*SQRT(L)

FINISH ! Exit post-process module

```

4.2 Workbench Optimization

First, a Mechanical APDL component is added to the Project Schematic by dragging it from the Component Systems menu. The APDL code is then imported into Workbench. Next, from among all the properties defined in the APDL script, the *input* (G_{Ic} , G_{IIc}), and *output* D are selected.

Optimization techniques are used in this study to minimize the error (16) by adjusting

Table 5: Error for all laminates considered, calculated by Response Surface (RS) and Design Optimization (DO).

Laminate	Error D		
	RS	DO	(RS-DO)/DO
#1	0.002986	0.002937	2%
#2	0.004918	0.005179	-5%
#3	0.005769	0.005891	-2%
#4	0.01155	0.011797	-2%
#5	0.01384	0.01466	-6%
#6	0.03584	0.037435	-4%
#7	0.002859	0.004631	-38%
#8	0.025511	0.026829	-5%
#9	0.011437	0.009954	15%

the input (material properties) to minimize the *output* (error). A Response Surface Optimization (RSO) component is now added to the Workbench project by dragging it from the Component Systems menu to the Project Schematic.

Then, DoE is used to adjust a multivariate quadratic polynomial to the actual response (objective) of the system as defined by the APDL script. In this study the objective is the error D in (16) and the multivariate are the properties G_{Ic} and G_{IIc} . Then, the RS is used to plot the objective D vs. each of the properties and to calculate the sensitivities. This allows the user to select, for optimization, only the properties to which the objective (error) is sensitive. This varies from one laminate to another.

Within RSO, optimization is performed by using the RS rather than actual evaluation of the response via finite element analysis (FEA). This results in significant savings of computer time, as shown in Table 1, but the result is approximate because the RS is an approximation to the actual objective function. To get exact optimum properties (within numerical accuracy) one has to conduct Direct Optimization (DO). It can be seen in Table 5 that RS is quite accurate when compared with DO, considering that the number of FEA evaluations (reported in Table 1) is smaller for RS than for DO.

As it is shown in Table 6, the accuracy of the properties is good when RS is used instead of DO. A cost comparison, in terms of number of FEA evaluations, is shown in Table 1, where it can be seen that DO is much more expensive.

Twenty two experimental data points are available for laminate #1 and nineteen experimental data points are available for laminate #8. Laminate #1 $[0_2/90_4]_S$ was chosen because this laminates is sensitive to G_{Ic} . On the contrary, G_{IIc} does not have any effect on the results of Laminate #1, as shown in Figure 4.

For minimizing the error D, lower and upper limits must be chosen for each input (Table 3). Since the response surface is approximate (performing actual evaluation via FEA for

Table 6: Comparison of adjusted input (material) parameters obtained by using Response Surface Optimization (RSO) and Direct Optimization (DO).

Parameter	Units	Optimization method	
		RSO (Response Surface)	DO (Adaptive Single-Objective)
G_{IC}	kJ/m^2	0.4285	0.4370
G_{IIC}	kJ/m^2	0.9660	1.0205
Max # of FEM evaluations		9	21

only a few points), direct optimization is used to check for accuracy. Direct optimization performs FEA at more points to iteratively construct increasingly refined response surfaces to be explored by the optimization algorithm. Results from response surface and direct optimization are compared in Table 6.

Since value of G_{IC} is found with laminate #1, the only property that remains to be found is G_{IIC} . For this purpose, laminate #8 $[0/\pm 40_4/0_{1/2}]_S$ is chosen because it experiences shear stress in the ± 40 laminas. In this way, G_{IIC} has a visible effect on the error D , as shown in Table 3.

Predicted laminate modulus $E_x(\epsilon_x)$ with properties listed in Table 6 are compared with experimental data for all the laminates. The error for each laminate is reported in Table 5.

5 Results

5.1 Other laminates

In this section, the material properties G_{IC} , G_{IIC} , determined earlier are used to predict the response of other laminates made with different laminate stacking sequence. The difference between predicted and experimental data for all nine laminates are reported in Table 5. Only laminates #1 and #8 were used to adjust the material properties. The modulus reduction of the remaining laminates (2–7, and 9) were calculated using those material properties. The error (Table 5) is very small for all laminates, demonstrating both the ability of the proposed procedure to adjust the material properties adequately and the ability of DDM to use those properties to accurately predict the modulus reduction of a variety of laminates (listed in Table 2).

5.2 Comparison with Other Models

In this section, results are compared with predictions using Progressive Damage Analysis (PDA), which is available in ANSYS. PDA uses three material properties: two strengths values (F_{2t} and F_6) and one dissipation energy (G_c). These properties were adjusted using

a variation of the procedure presented in this work. Laminate #1 was used to obtain $F_{2t} = 78.55$ MPa and $G_c = 27.50$ kJ/m². Laminate #8 was used to obtain $F_6 = 88.0$ MPa.

Since PDA uses only a single value of energy dissipation, predictions of damage evolution are accurate and comparable to those of DDM as long as one mode, say mode I, dominates. This can be observed for laminates #1 through #5, as shown in Figures 2, 5, and 6. All these laminates are subject to pure mode I crack opening in the 90-deg cluster. Also note that the cracking cluster is always composed of 8 plies. By adjusting F_{2t} and G_c with laminate #1, the analyst can obtain good predictions with PDA as long as the damage is dominated by mode I and the cracking cluster has the same thickness as the one used for adjusting F_{2t} .

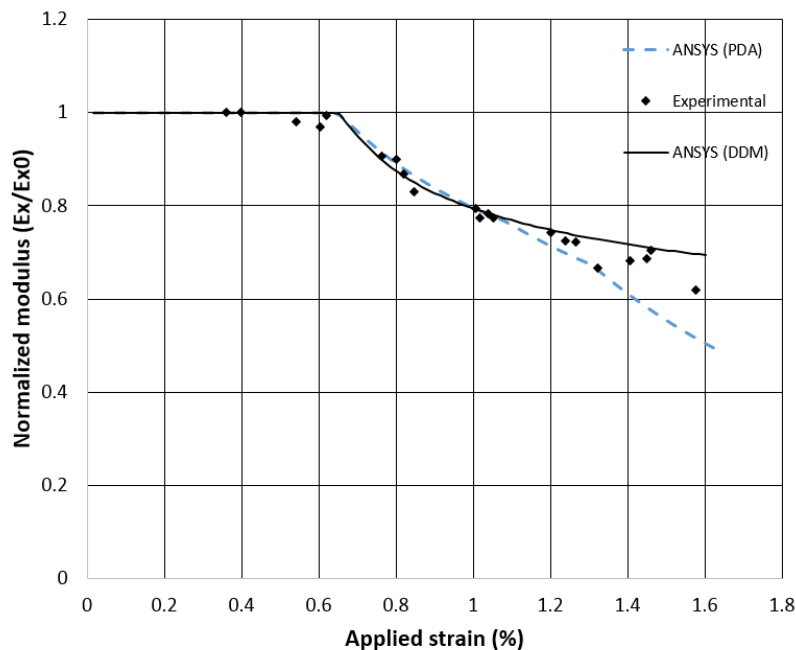


Figure 5: Normalized modulus vs. applied strain for laminate #3 (Table 2).

If the cracking cluster has a different thickness, the in situ strength will be different than F_{2t} . In fact, the in situ strength is inversely proportional to the square root of the cluster thickness [25, (7.42)]. In PDA, the transverse tensile strength F_{2t} and in-plane shear strength F_6 cannot be corrected for in situ effect, leading to errors when the properties have been adjusted with one value of lamina thickness but used to predict damage initiation for a different value of lamina thickness. Note that the cracking cluster in laminates #6 through #9 contain 4 plies (see Table 2), but F_{2t} has been adjusted with laminate #1, which has a cracking cluster that is twice as thick. This seems to be the reason for the discrepancy between PDA results and experimental data in Figures 7 and 8.

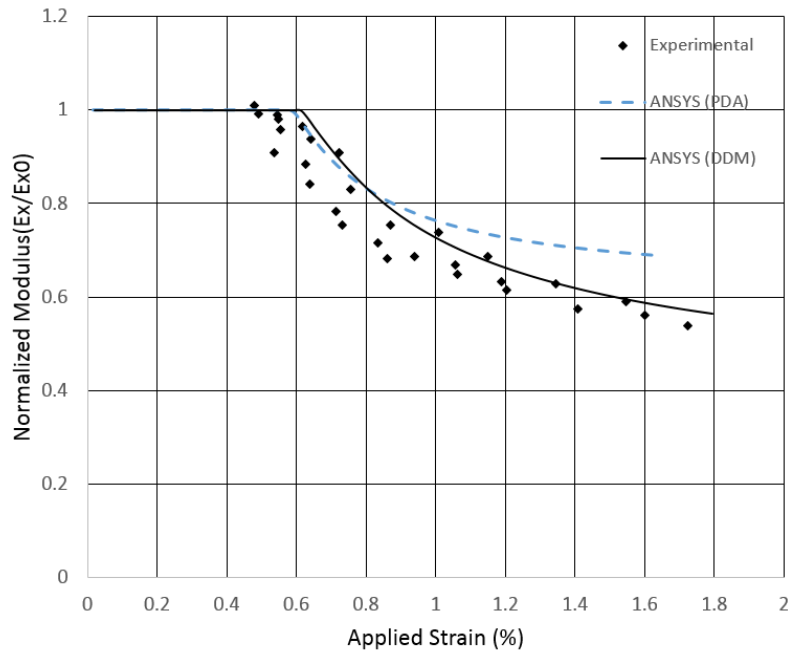


Figure 6: Normalized modulus vs. applied strain for laminate #5 (Table 2).

Since DDM automatically takes into account in situ strength, it is able to predict well the damage initiation regardless of the thickness of the cracking lamina or cluster. Damage evolution is also predicted correctly because DDM uses an interactive damage initiation and evolution criterion (1), that includes interaction between the two modes of crack propagation via two properties (G_{Ic} and G_{IIc}). DDM does not use strength for predicting crack initiation but simply the Griffith's criterion. Note that formulas for predicting in situ strength are based on Griffith's criterion [38].

5.3 Crack Density

As shown in the previous section, DDM can predict modulus reduction, but it also can predict crack density (number of cracks per unit length) as a function of applied load or strain. Comparison of predicted vs. experimental crack density are shown in Figures 9–10. It must be noted that DDM first calculates the reduced modulus matrix $[Q(\lambda)]$ of the laminate using an analytical solution of the elasticity equations over the RVE shown in Figure 1. Then, it calculates the crack density required to equilibrate the applied load. Thus, the quality of the modulus reduction is as good or better than that of the crack density.

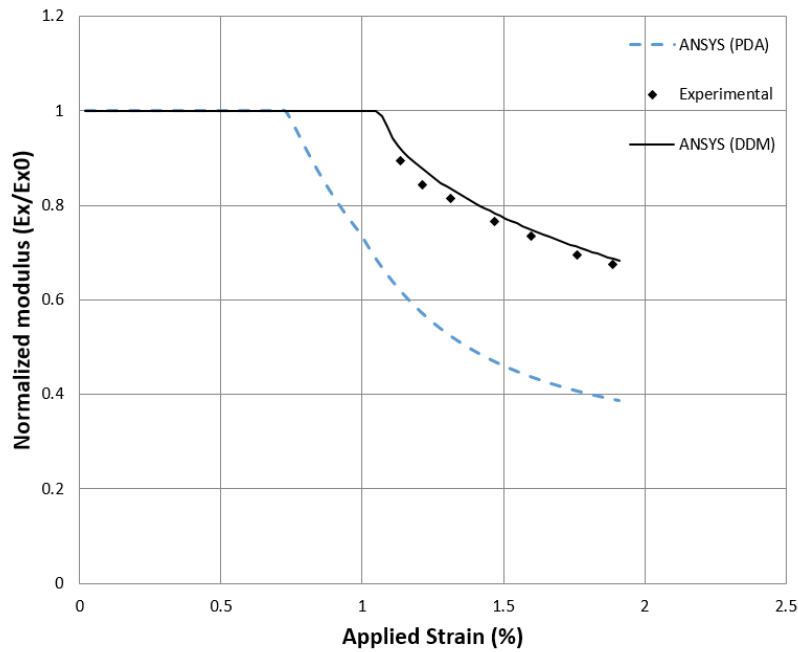


Figure 7: Normalized modulus vs. applied strain for laminate #7 (Table 2).

5.4 Mesh Sensitivity

Mesh sensitivity refers to how much the solution changes with element size, number of elements, or number of nodes. It can be seen in Figures 11-12 that DDM results are not sensitive number or type of elements, i.e. to mesh density.

Mesh density refers to the number of nodes, number of elements, and element type (linear or quadratic) used to discretize the domain. Mesh density affects the solution in two ways: (a) convergence and (b) objectivity. As the mesh density increases, FEA is able to approximate the strain gradients in the solution, asymptotically to a final value. Once the strain distribution on the domain is close to the asymptotic value, the solution does not change appreciably due to further refinement of the mesh. This is called convergence of the solution. Next, objectivity deals with the accuracy of the converged solution, which can be investigated as follows. For a problem for which the exact solution predicts a constant strain in the entire domain, the solution should be absolutely independent of mesh refinement. That is, a one-element mesh should provide the same result as an n -element mesh for any value of n . If it does not, it is an indication of lack of objectivity of the constitutive model, as it is shown in [39] for a different damage model. Lack of objectivity means that the constitutive model returns a different estimate of the stress corresponding to a given strain, depending on the size of the element and/or element type (linear or quadratic).

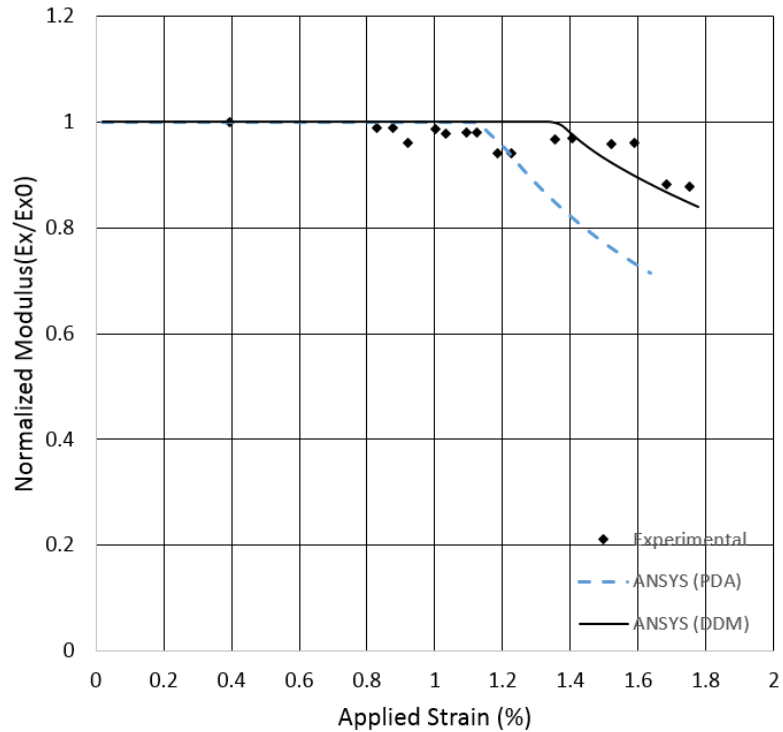


Figure 8: Normalized modulus vs. applied strain for laminate #9 (Table 2).

The solution may still converge in the sense of (a), but to an incorrect value.

Since the results in this study are for rectangular specimens subjected to uniaxial load, there is no strain gradient (the strain is constant over the entire model). Therefore, a single element should provide the same strain, stress, and damage results accurately. It is shown in Figures 11 and 12 that this is true regardless of the number of elements or element type used (PLANE 182 or PLANE 183).

6 Conclusions

A novel methodology is proposed to determine the material parameters for Discrete Damage Mechanics in ANSYS and the procedure is explained in detail.

It is observed that adjusted material properties G_{IC} , G_{IIC} , can be used to predict crack initiation and evolution using ANSYS, and that good comparison with available experimental data for different laminates is achieved.

DDM not only predicts modulus reduction but also crack density as a function of load or applied strain. Unlike classical damage variables based on modulus reduction, crack

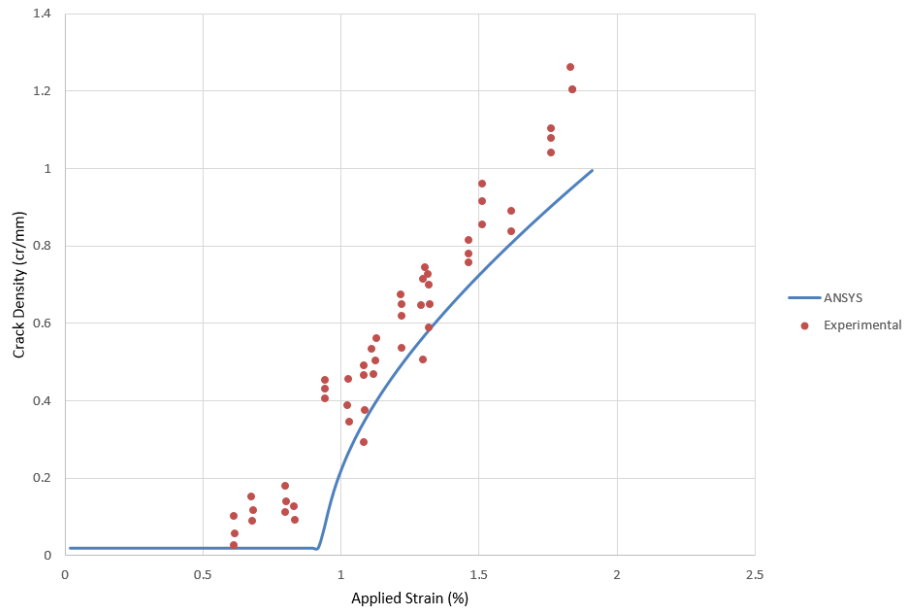


Figure 9: Crack density vs. strain for laminate #6 (Table 2).

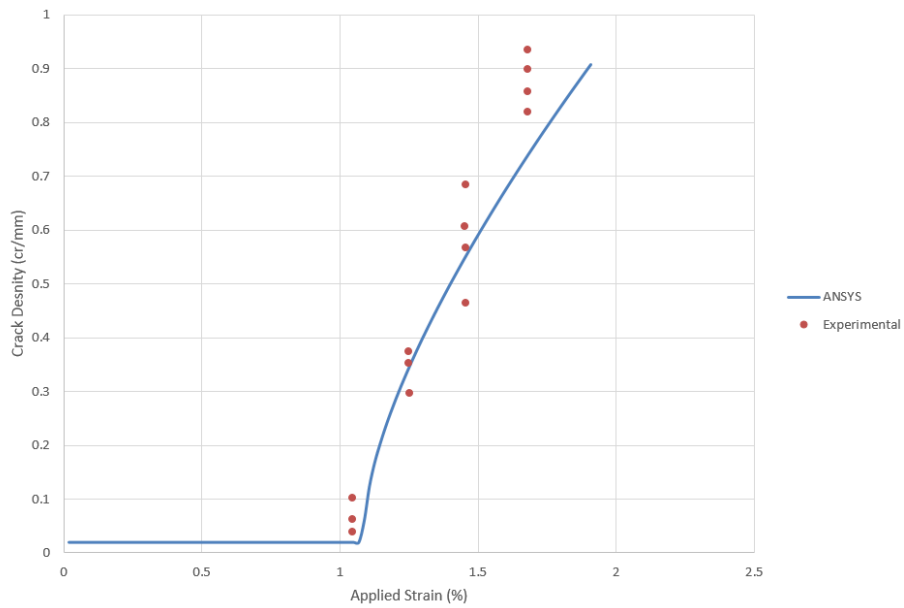


Figure 10: Crack density vs. strain for laminate #7 (Table 2).

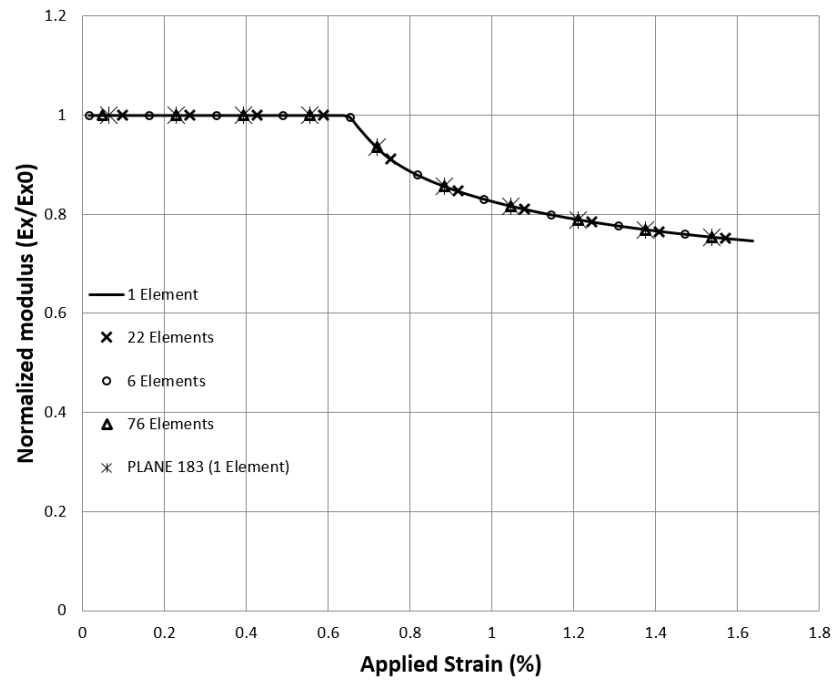


Figure 11: Normalized Modulus vs. applied strain for laminate #1 using different number of elements for PLANE 182 and one element for PLANE 183.

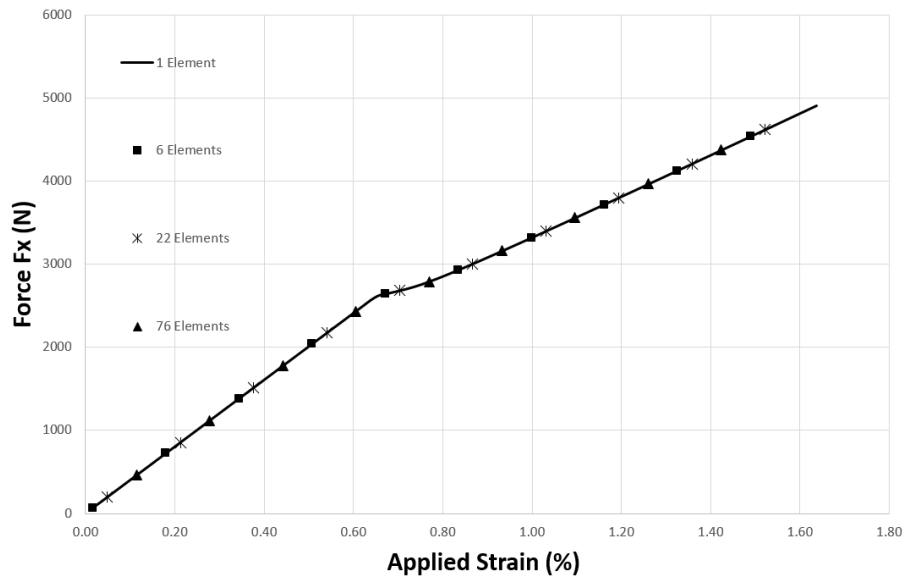


Figure 12: Reaction force vs. applied strain for laminate #1 using different number of elements (PLANE 182).

density is a true (measurable) state variable, which additionally could be correlated with the permeability of the composite.

ANSYS/DDM is shown to be independent of mesh density, element type and size, and number of nodes.

When compared to PDA, DDM provides better predictions for laminates containing angle-ply clusters because DDM has an independent parameter, namely G_{IIc} , to model the shear component of cracking, while PDA does not. Furthermore, DDM can better predict damage initiation because it does not need strength values, which are susceptible to in situ effect. Instead DDM uses the critical ERR's parameters to predict both initiation and evolution of cracking.

When compared to direct optimization methods, response surface demonstrates two advantages. First, it allows for fast computation of the sensitivity of the error to the material properties sought, thus allowing the analyst to select the most appropriate laminate stacking sequence to adjust each material property. Second, RS is able to adjust the material properties accurately and with low computational expense. However, the direct optimization method is always available to perform a final check.

Acknowledgments

The authors acknowledge the infrastructure support from the Energy Materials Science and Engineering (EMSE) program at West Virginia University.

References

- [1] P Ladevèze, O Allix, J F Deü, and D Lévêque. A mesomodel for localisation and damage computation in laminates. In *Computer Methods in Applied Mechanics and Engineering*, volume 183, pages 105–122, 2000.
- [2] E Abisset, F Daghia, and P Ladevèze. On the validation of a damage mesomodel for laminated composites by means of open-hole tensile tests on quasi-isotropic laminates. *Composites Part A*, 42(10):1515–1524, 2011.
- [3] F Rastellini, S Oller, and O Salomon E Onate. Composite materials non-linear modelling for long fibre-reinforced laminates continuum basis computational aspects and validations. *Computers & Structures*, 86(9):879–896, 2008.
- [4] X Martinez and S Oller. Numerical simulation of matrix reinforced composite materials subjected to compression loads. *Archives of computational methods in engineering*, 16(4):357–397, 2009.
- [5] X Martinez, F Rastellini, S Oller, F Flores, and E Onate. Computationally optimized formulation for the simulation of composite materials and delamination failures. *Composites Part B*, 42(2):134–144, 2011.
- [6] R J Nuismer and S C Tan. Constitutive relations of a cracked composite lamina. *Journal of Composite Materials*, 22(306):306–321, 1988.
- [7] S C Tan and R J Nuismer. A theory for progressive matrix cracking in composite laminates. *Journal of Composite Materials*, 23:1029–1047, 1989.
- [8] E Adolfsson and P Gudmundson. Matrix crack initiation and progression in composite laminates subjected to bending and extension. *International Journal of Solids and Structures*, 36:3131–3169, 1999.
- [9] J M Berthelot. Transverse cracking and delamination in cross-ply glass-fiber and carbon-fiber reinforced plastic laminates: static and fatigue loading. *Applied Mechanics Review*, 56:111–147, 2003.
- [10] S H Lim and S Li. Energy release rates for transverse cracking and delaminations induced by transverse cracks in laminated composites. *Composites Part A*, 36(11):1467–1476, 2005.

- [11] D T G Katerelos, M Kashtalyan, C Soutis, and C Galiotis. Matrix cracking in polymeric composites laminates: Modeling and experiments. *Composites Science and Technology*, 68:2310–17, 2008.
- [12] A. Adumitroaie and E. J. Barbero. Intralaminar damage model for laminates subjected to membrane and flexural deformations. *Mechanics of Advanced Materials and Structures*, 22(9):705–716, 2015.
- [13] J. A. Nairn. *Finite Fracture Mechanics of Matrix Microcracking in Composites. Application of Fracture Mechanics to Polymers, Adhesives and Composites*. Elsevier, 2004.
- [14] D T G Katerelos, J Varna, and C. Galiotis. Energy criterion for modeling damage evolution in cross-ply composite laminates. *Composites Science and Technology*, 68:2318–24, 2008.
- [15] A Matzenmiller, J Lubliner, and R. Taylor. A constitutive model for anisotropic damage in fiber-composites. *Mechanics of Materials*, 20:125–152, 1995.
- [16] P Camanho and C Davila. Mixed-mode decohesion finite elements for the simulation of delamination in composite materials. In *NASA TM 2002-211737*, pages 1–37, 2002.
- [17] Firehole Composites. Helius mct composite materials analysis software. 2016. <http://www.firehole.com/products/mct/>.
- [18] Alpha STAR Corporation. Genoa virtual testing & analysis software,. 2016. <http://www.ascgenoa.com>.
- [19] ANSYS. *Mechanical APDL, Advanced Analysis Guide, 9. User-Programmable Features*. SAS IP, Inc, 17.1 edition, 2016.
- [20] E. J. Barbero. *Finite Element Analysis of Composite Materials Using ANSYS*. CRC Press, 2nd edition, 2014.
- [21] ANSYS. *DesignXplorer User’s Guide*. SAS IP, Inc, 17.1 edition, 2016.
- [22] J. Varna, R. Joffe, N.V. Akshantala, and R. Talreja. Damage in composite laminates with off-axis plies. *Composites Science and Technology*, 59(14):2139–2147, 1999.
- [23] J. Varna, R. Joffe, and R. Talreja. A synergistic damage-mechanics analysis of transverse cracking [/904]s laminates. *Composites Science and Technology*, 61(5):657–665, 2001.
- [24] E. J. Barbero and D. H. Cortes. A mechanistic model for transverse damage initiation, evolution, and stiffness reduction in laminated composites. *Composites Part B*, 41:124–132, 2010.

- [25] E. J. Barbero. *Introduction to Composite Materials Design*. CRC Press, 2 edition, 2011.
- [26] H.T. Hahn. A mixed-mode fracture criterion for composite materials. *J. Compos. Technol.. Research*, 5:26–29, 1983.
- [27] E. J. Barbero and F. A. Cosso. Determination of material parameters for discrete damage mechanics analysis of carbon-epoxy laminates. *Composites Part B*, 56:638–646, 2014.
- [28] D. Bruno, F. Greco, and P. Lonetti. A 3d delamination modelling technique based on plate and interface theories for laminated structures. *European Journal of Mechanics A/Solids*, 24:127–149, 2005.
- [29] E. J. Barbero, G. Sgambitterra, A. Adumitroiaie, and J. Martinez. A discrete constitutive model for transverse and shear damage of symmetric laminates with arbitrary stacking sequence. *Composite Structures*, 93:1021–1030, 2011.
- [30] E. J. Barbero, G. Sgambitterra, and A. Tessler. A robust three-node shell element for laminated composites with matrix damage. *Composites Part B: Engineering*, 42:41–50, 2011.
- [31] E. J. Barbero, F. A. Cosso, and X. Martinez. Identification of fracture toughness for discrete damage mechanics analysis of glass-epoxy laminates. *Applied Composite Materials*, November:1–18, 2013.
- [32] E. J. Barbero and F. A. Cosso. Benchmark solution for degradation of elastic properties due to transverse matrix cracking in laminated composites. *Composite Structures*, 98:242–252, 2013.
- [33] M. M. Moure, S. Sanchez-Saez, E. Barbero, and E. J. Barbero. Analysis of damage localization in composite laminates using a discrete damage model. *Composites Part B*, 66:224–232, 2014.
- [34] M.M. Moure, F. Otero, S.K. Garcia-Castillo, S. Sanchez-Saez, E. Barbero, and E. J. Barbero. Damage evolution in open-hole laminated composite plates subjected to in-plane loads. *Composite Structures*, 133:1048–1057, 2015.
- [35] M. Ghayour, H. Hosseini-Toudeshky, M. Jalalvand, and E. J. Barbero. Micro/macro approach for prediction of matrix cracking evolution in laminated composites. *Journal of Composite Materials*, 0(0):1–13, 2015.
- [36] M.M. Moure, S.K. Garcia-Castillo, S. Sanchez-Saez, E. Barbero, and E. J. Barbero. Influence of ply cluster thickness and location on matrix cracking evolution in open-hole composite laminates. *Composites Part B: Engineering*, 95:40–47, 2016.

- [37] E. J. Barbero. UserMAT.DLL Release 14, 2013. <http://barbero.cadec-online.com/feacm-ansys>.
- [38] G. J. Dvorak and N. Laws. Analysis of progressive matrix cracking in composite laminates – II first ply failure. *J. Compos. Mater.*, 21:309–329, 1987.
- [39] E. J. Barbero, F. A. Cosso, R. Roman, and T. L. Weadon. Determination of Material Parameters for Abaqus Progressive Damage Analysis (PDA) of E-Glass Epoxy Laminates. *Composites Part B:Engineering*, 46:211–220, 2013.